

1 **Temporary stratification promotes large greenhouse gas emissions in a shallow eutrophic lake**

2 Thomas A Davidson^{1,2,-}, Martin Søndergaard^{1,2,3}, Joachim Audet^{1,2}, Eti Levi¹, Chiara Esposito^{1,2}, Tuba
3 Bucak Onay¹, Anders Nielsen^{1,4}.

4

5 ¹ Lake Ecology, Department of Ecoscience, Aarhus University, Denmark

6 ² WATEC Aarhus University Centre for Water Technology, Aarhus University, Denmark

7 ³ Sino-Danish Centre for Education and Research (SDC), Beijing, China

8 ⁴ WaterITech Aps, Døjsøvej 1, 8660 Skanderborg, Denmark

9 Corresponding author: Thomas A Davidson, Department of Ecoscience, Aarhus University, C. F. Møllers

10 Alle 4-6, DK-8000 Aarhus C, Denmark, e-mail: thd@ecos.au.dk

11

12

13

14

15

16 **Abstract**

17 Shallow lakes and ponds undergo frequent temporary thermal stratification. How this affects greenhouse
18 gas (GHG) emissions is moot, with both increased and reduced GHG emissions hypothesised. Here,
19 weekly estimation of GHG emissions, over growing season from May to September, were combined with
20 ~~high-resolution~~ temperature and oxygen profiles of an 11 hectare temperate shallow lake to investigate
21 how thermal stratification shapes GHG emissions. There were three main stratification periods with
22 profound anoxia occurring in the bottom waters ~~occurring quickly~~ upon isolation from the atmosphere.
23 Average diffusive ~~emission~~emissions of methane (CH₄) and nitrous oxide (N₂O) were larger and more
24 variable in the stratified phase, whereas carbon dioxide (CO₂) was on average lower. ~~CH₄ ebullition was~~
25 ~~an, though these differences were not statistically significant. In contrast, there was a significant,~~ order of
26 magnitude ~~greater, increase~~ in CH₄ ebullition in the stratified phase. ~~In addition~~ Furthermore, at the end of
27 the period of stratification, there was a large efflux of CH₄ and CO₂ ~~whenas~~ the lake mixed ~~mixed after~~
28 ~~periods of extended (circa 14 days) thermal stratification. These two. Two relatively isolated~~ turnover
29 events were estimated to have released the majority of the CH₄ emitted between May and September.
30 These results demonstrate how stratification patterns can shape GHG emissions and highlight the role of
31 turnover emissions ~~resulting from temporary thermal stratification and also~~ and the need for high
32 frequency measurements of GHG emission ~~in order~~ which are required to accurately characterise
33 emissions, particularly from ~~these~~ temporarily stratifying lakes.

34

35

36 Keywords: Climate change; lake stratification; methane; carbon dioxide; nitrous oxide; climate
37 feedbacks

38

39 1. Introduction

40 Fresh waters are key sites for the processing of greenhouse gases (GHG), methane (CH₄), carbon dioxide
41 (CO₂) and nitrous oxide (N₂O). Shallow lakes, in particular, have been identified as hot spots of CH₄
42 release, particularly when ebullition is taken into account (Davidson et al., 2018; Aben et al., 2017). The
43 certainty that fresh waters are large emitters of GHGs contrasts with the uncertainties associated with the
44 quantities emitted and this is in large part due to historical paucity of measurements (Cole, 2013). ~~A~~
45 ~~recent study identified the highly variable emissions from lakes and ponds which make a large 40~~
46 ~~proportion of total emissions (Rosentreter et al., 2021). A dearth of measurement combined with these A~~
47 recent study identified the highly variable emissions from lakes and ponds which contribute to more than
48 half the total emissions (Rosentreter et al., 2021). Whilst different morphometric features and chlorophyll-
49 a explained some of the emission patterns (Deemer and Holgerson, 2021), it is also clear that a dearth of
50 measurement combined with these highly variable emissions makes determining the drivers and controls
51 of those emissions a challenge, which in turn makes predicting future emissions difficult.

52
53 The current and future effects of climate change on lakes in general and on their GHG emissions are
54 relevant questions as there is potential for positive feedbacks and synergies with other human impacts
55 such as eutrophication (Davidson et al., 2018; Beaulieu et al., 2019; Delsontro et al., 2016; Meerhoff et
56 al., 2022). Taking a broad metabolic theory of ecology approach, temperature increases should promote
57 methanogenesis and shift the balance from primary production to respiration increasing CO₂ emission at
58 cellular and ecosystem scale (Yvon-Durocher et al., 2010). However, empirical and experimental data
59 indicate that temperature is not the sole control of primary production and methanogenesis. In particular,
60 eutrophication, and the promotion of large algal crop, has been associated with increased emissions of
61 CH₄ and N₂O (Delsontro et al., 2016) both by diffusion and ebullition (Zhou et al., 2019). Furthermore, in
62 what is globally the most abundant lake type, small shallow lakes, where macrophytes can colonise large
63 areas of the lake bed, ~~thus~~ trophic state and the dominance of submerged plants or algae may be more

64 important than temperature in shaping GHG dynamics (Davidson et al., 2015; Davidson et al., 2018;
65 Bastviken et al., 2023).

66

67 Climate change effects on lakes are not limited to increases in average temperatures and lengthening of
68 the growing season. Increases in both the frequency and intensity of heat waves are predicted, which will
69 promote the warming of surface waters and in turn make permanent and temporary thermal stratification
70 of lakes more likely (Woolway and Merchant, 2019), even in lakes typically classified as non-stratifying
71 (Kirillin and Shatwell, 2016). A recent study Holgerson et al. (2022) identified stratification and mixing
72 patterns in small water bodies, with permanent summer stratification common and frequent mixing
73 occurring in larger standing waters (>4 ha) lakes. Such periods of stratification and mixing events are
74 likely to have profound effects on GHG dynamics. Emissions of gases, in particular CH₄, that accumulate
75 in the isolated bottom waters of a stratified lake, occurs upon mixing and can make very significant
76 contributions to cumulative emissions (Schubert et al., 2012). High-resolution studies of sites that
77 undergo temporary stratification are, however, rare (Søndergaard et al., 2023). In terms of its effects on
78 GHG dynamics, there are potentially antagonistic processes at work in a stratified lake. On the one hand
79 the ‘shield effect’ results in lower temperatures at the sediment surface slowing down metabolic processes
80 that scale with temperature, i.e. methanogenesis and mineralization of organic carbon (C), reducing
81 emission and promoting C burial. On the other hand, anoxia at the sediment surface may shift processes
82 towards fermentation, increasing the proportion and total amount of CH₄ produced and perhaps reducing
83 C burial (Bartosiewicz et al., 2019). Recent work combining empirical observations and models has
84 suggested that shielding effects are larger than the anoxia effects and that stratification, in general,
85 increases C burial and reduces GHG emissions. ~~The stratification induced isolation of bottom waters was~~
86 ~~reported to lead to reduced ebullition of CH₄ and a shift to diffusive pathways~~ (Bartosiewicz et al., 2015).
87 The stratification induced isolation of bottom waters was reported to lead to reduced ebullition of CH₄
88 and a shift to diffusive pathways. It might, however, be predicted that in shallow lakes stratification
89 would lead to much larger CH₄ release as anoxic conditions would limit CH₄ oxidation by CH₄ oxidizing

90 bacteria (MOBs) (Bastviken et al., 2008). There may also be other factors with the potential to increase
91 GHG emission, such as sediment organic content and lake trophic status (Delsontro et al., 2016), which
92 may interact with stratification patterns in shaping GHG emissions.

93

94 In this study, we used data from a shallow lake with high frequency measurements of temperature profiles
95 combined with weekly measurements of dissolved gas concentrations in the surface and bottom waters
96 and continuous measurement of ebullitive emissions of CH₄ to track the effects of lake stratification on
97 GHG emissions. The key question was how ebullitive and diffusive fluxes of the key GHGs: CH₄, CO₂
98 and N₂O respond to temporary thermal stratification.

99

100 **2. Materials and methods.**

101 **2.1 Study site**

102 Ormstrup lake, located in Denmark (lat 56.326°, lon 9.639°) (Fig.1) (depth map with GHG sampling
103 locations), is an 11 ha, shallow lake (average depth 3.4 m), with a maximum depth of 5.5 m, and with a
104 relatively long hydraulic retention time (> 1 year). The lake is eutrophic with high TP and chlorophyll-a
105 (Table 1; Søndergaard et al., 2022) with very sparse occurrence of submerged plants.

106

107 **2.2 Depth profiling and high frequency measurements**

108 In June 2020, a Nexsens (NexSens Technology, Fairborn, OH, USA) CB-450 data buoy system
109 (https://www.nexsens.com/pdf/CB450_datasheet.pdf) was deployed at the deepest point of the lake
110 equipped with a Nexsens TS210 thermistor string https://www.nexsens.com/pdf/TS210_datasheet.pdf
111 with temperature nodes measuring at 4 levels; one sensor “in air”, ca. 5 cm above the water surface, (but
112 shielded from direct light), and three sensors at -1, -2, -3 meters, respectively relative to the water surface.
113 In addition two Aqua TROLL 500 (In-Situ, Fort Collins, CO, USA) multi-sondes were mounted near the

114 surface (-1.0 meters) and at deeper water depth (-3.8 meters). The near surface and deeper water sonde
115 were configured with sensors to measure dissolved oxygen (DO) and water temperature (Tw). The optical
116 sensors were calibrated according to manufacture guidelines and checked on a weekly basis.

117
118 The optical sensors of the Aqua TROLL 500 have a built-in wiper mechanism to clean sensor heads to
119 hamper bio-fouling. The wiper function was enabled to perform cleaning in sync with sensor
120 measurements, hence every 15 minutes. In addition, manual cleaning of sensor heads was done every
121 week, while routine manual field monitoring was carried out at the lake. Prior to the deployment of the
122 buoy, and as a validation exercise for the buoy data, weekly manual profiles of DO and Tw were collected
123 at the deepest point.

124
125 Periods of stratification were defined by a greater than 2 °C difference between the surface and bottom
126 waters and DO below 0.5 mg l⁻¹ at the time of the weekly manual profiling of the system. The high
127 frequency measurements were used to confirm the patterns. During periods of defined as stratified, there
128 were partial mixing events where the depth of the thermocline and oxycline change and there was some
129 mixing of the bottom waters and surface waters. of the water column mixes, ~~but~~whilst the bottom waters
130 ~~remain~~remained undisturbed. ~~as the DO did not increase the partial mixing above might increase gas~~
131 exchange.

132

133 **2.3 Water chemistry**

134 Water samples for the analysis of Chlorophyll-a were collected weekly from the 20. April 2020 from
135 surface (-0.5 m) water at station 3 (Fig. 1) ~~and analysed according to Danish standard procedures~~
136 (Søndergaard et al., 2005). 1). A volume of water ranging from (0.2 to 1 litre) was filtered and the GFC
137 papers preserved for chlorophyll-a analysis, which were determined spectrophotometrically after ethanol
138 extraction (Jespersen and Christoffersen, 1987) ~~and -alkalinity was measured weekly by gran titration~~

139 (Søndergaard et al., 2005). Depth profiles of temperature, electrical conductivity (EC) and dissolved
140 oxygen (DO) were measured manually with an Aqua TROLL 500 probe from every -0.5 or -1 m down to
141 -5 m depth).

142

143 **2.4 Greenhouse gas sampling**

144 2.4.1 Dissolved concentration

145 Samples of dissolved concentrations of CH₄, CO₂ and N₂O were collected weekly from the 20. April 2020
146 from surface waters and weekly from surface and bottom water from the 26. May 2020. The samples
147 were taken using head-space equilibration after (Mcauliffe, 1971), where 20 ml of water was collected
148 from just below the water surface and 20 ml of N₂ was introduced as a headspace in a 60-ml syringe and
149 then shaken vigorously for one minute. The 20 ml headspace was then transferred to a 12-ml pre
150 evacuated glass vial.

151

152 ~~Samples were collected between 12. May 2020–15. October 2020 which is 126 days and cover the majority~~
153 ~~of the growing season.~~

154 Gas concentrations in the headspace were determined on a dual-inlet Agilent 7890 GC system interfaced
155 with a CTC CombiPal autosampler (Agilent, Nærum, Denmark) (Petersen et al., 2012). For the GC,
156 certified CO₂, CH₄ and N₂O standards were used for calibration and validation. Aqueous concentrations in
157 N₂O, CH₄ and CO₂ were calculated from the headspace gas concentrations according to Henry's law and
158 using Henry's constant corrected for temperature and salinity (Weiss, 1974; Weiss and Price, 1980;
159 Wiesenburg and Guinasso, 1979). A recent study (Koschorreck et al., 2021) identified significant bias in
160 the estimate of CO₂ concentrations using headspace equilibration at lower concentrations. We applied their
161 correction using separately measured alkalinity as described in Koschorreck et al. (2021).

162 The fluxes of N₂O, CH₄ and CO₂ between the water and the overlying atmosphere were estimated as

163

$$f_g = k_g(C_{wat,g} - C_{eq,g})$$

164 Where f_g is the flux of a specific gas g , k_g is the piston velocity of the gas and $C_{wat,g} - C_{eq,g}$ is the
165 gradient of concentration between the concentration of gas dissolved in the water ($C_{wat,g}$) and the
166 concentration of gas the water would have at equilibrium with the atmosphere ($C_{eq,g}$).
167 We calculated a gas transfer velocity k_{600} for each sampling occasion using the relationship based on
168 windspeed described in (Cole and Caraco, 1998).

$$k_{600} = 2.07 + 0.215U_{10}^{1.7}$$

170 U_{10} is the mean daily windspeed at 10m ($m s^{-1}$) obtained from the Danish meteorological institute
171 (DMI;20x20 km grid data)

$$k_g = k_{600} \left(\frac{Sc_g}{600} \right)^x$$

174
175
176 Sc_g is the Schmidt number(Wanninkhof, 1992) of the specific gas g . We chose $x = -2/3$ as this factor is
177 used for smooth liquid surface (Deacon, 1981).

178
179 Daily flux rates were calculated using linear interpolation of the weekly surface measurements from each
180 of the sampling points. The diffusive surface water fluxes were calculated by taking an average of the daily
181 flux rate from the 12. May 2020 to the 13. October 2020 for each location. Then an average of the 3 locations
182 was multiplied by the area of the lake and the number of days covered by the study, here 126 days was
183 chosen to match the period over which ebullition was measured.

184
185 The total content of the gases in the lake's bottom waters were calculated from the concentration of the
186 ~~165 gases per litre multiplied by an estimate of the volume of the water in the hypolimnion. The volume~~
187 ~~of 166 water in the hypolimnion was estimated from the lake profiles manually conducted on the day of~~
188 ~~167 sampling. The top of the hypolimnion was determined by the depth below which oxygen was less~~

189 ~~than 0.5 168 mg l⁻¹. A detailed bathymetry of the lake allows the calculation of the area and therefore~~
190 ~~volume of water 169 that lies below a given depth. For the purposes of this study, it was assumed that all~~
191 ~~the gas in the 170 hypolimnion was released on turnover. This release was calculated from 30. June 2020~~
192 ~~and from the 25. 171 August 2020, as they are the periods where complete mixing occurred and all the~~
193 ~~gases accumulated in 172 the bottom waters was likely to be released~~gases per litre multiplied by an
194 estimate of the volume of the water in the hypolimnion. The volume of water in the hypolimnion was
195 estimated from the lake profiles manually conducted on the day of sampling. The top of the hypolimnion
196 was determined by the depth below which oxygen was less than 0.5 mg l⁻¹. A detailed bathymetry of the
197 lake allows the calculation of the area and therefore volume of water that lies below a given depth.

198

199 During the study period two major turnover events occurred, the process of lake turnover and full mixing
200 can take a number of days, and the outgassing even longer. The oxygen data, from the buoy, indicated
201 that it can take up to four days and this provides time for CH₄ oxidation to occur (Søndergaard et al.,
202 2023). In order to estimate the amount of CH₄ oxidised over the course of the multiple days of degassing
203 we directly measured CH₄ oxidation rates in the surface waters of the lake. This was done in June 2023 in
204 five locations using methods outlined in (Thottathil et al., 2019) where five water samples from five
205 different locations and each was incubated over 4 days with and the change in CH₄ concentration used to
206 calculate oxidation rates. We used the minimum (0.267 µg CH₄-C l⁻¹ h⁻¹), mean (0.44 µg CH₄-C l⁻¹ h⁻¹)
207 and maximum (0.58 µg CH₄-C l⁻¹ h⁻¹) oxidation rates to estimate the range of CH₄ oxidation likely to have
208 occurred over the course of the two main turnover events. Assuming that the degassing took four days,
209 these rates would consume between 2 and 8% of the CH₄ contained in the hypolimnion. Using the mean
210 oxidation value the turnover fluxes were reduced by 4.1% on the 30th of June 2020 and by 6% for the 25th
211 August 2022.

212

213

214 2.4.2 Ebullition

215 The ebullitive flux of CH₄ was estimated using at total of 40 floating chambers placed on 4 transects of 10
216 chambers each (Fig. 1). The chambers have a volume of 8 litre and a surface area of 0.075 m², similar to
217 those used by (Bastviken et al., 2015). As the existing literature indicated that ebullition is lower as water
218 depth increases -(Wik et al., 2013) the transects were placed to maximise the measurement of the low end
219 of the depth gradient on the shallower slopes of the western end of the lake (Fig. 1). The average and
220 maximum -depth of each transect was T1: 293 cm and 472 cm; T2: 181 cm and 267, T3: 223 cm and 300
221 cm and T4 166 cm and 220 cm. The chambers were set on the 14. May 2020 and sampled every two
222 weeks from that date, and on one occasion after one week- until September 17th, which is a period of 127
223 days. Twenty ml of sample was taken from the floating chamber and injected into a pre-evacuated 12 ml
224 vial (exetainer, Labco). Gas concentrations were determined on the same GC than described above
225 (Petersen et al., 2012)

226 Ebullitive flux of CH₄ was estimated as:

$$227 \frac{p_{gas} \times Vol_{bub}}{t \times A}$$

228 Where p_{gas} is the concentration of CH₄ in the gas that was trapped, Vol_{bub} is the volume of the chamber
229 (i.e. 7L), t is the time during which the samples was collected and A is the area of chamber (i.e. 0.075 m²).

230 A portion of the CH₄ released via ebullition in the chamber will have re-dissolved in the water or might
231 leak through the chamber walls, thus underestimating the ebullitive flux. We have made a number of
232 measurements to constrain this error and to compare estimates based on static chambers with other
233 approaches. The result show that whilst static chambers underestimate ebullition, given the temporal
234 variability of ebullition, static chambers continually deployed provide a better estimate of average ebullition
235 than short term (24-48 hours) deployment using portable gas monitors or flushing chambers.

236
237 Therefore, whilst static chambers method cannot be said to accurately quantify CH₄ emissions, they can be
238 relied upon to compare differences in ebullition between time periods, with the caveat that they are always
239 an underestimate of actual ebullitive flux.

240

241 Total ebullitive flux from the lake was calculated by taking a mean of the emissions from each transect over
242 the 126 day period. Then taking an average of the means of four transects and multiplying this by the time
243 of deployment of the chambers in days, which was 126 days, and by the area of the lake. This gives a total
244 ebullitive flux of CH₄ for the lake over the period of measurement- from May to mid September.

245

246 The three different flux types, surface diffusion, ebullition and turnover emission were then converted in
247 comparable units of total lakes emissions (as g or kg of gas) over the studied period and also converted into
248 CO₂-equivalents using a conversion factor related to their 100 year global warming potential (GWP) of 28
249 for CH₄ and 298265 for N₂O.

250

251 2.5 Statistical methods

252 To test for a significant difference among the emissions from the stratified and mixed phase we used
253 generalised least squares (GLS) with a variance function to account for heterogeneity of variance between
254 the phases. In the case of the ebullitive flux, as the collected phase often covered periods including both
255 mixed and stratified phases there were three categories, mixed, stratified and both mixed and stratified.
256 All analysis was carried out in R version 4.2.1 (R Development Core Team, 2022) and the GLS used the
257 package nlme (Pinheiro et al., 2014).

258

259 **3.0 Results**

260 **3.1 Lake physical and chemical characteristics**

261 Depth profiles measured weekly from April show that stratification was initiated by the 26. May 2020 this
262 may have broken down briefly and established again, visible in the temperature sensors for the buoy on

263 the 5. June 2020 (Fig. 2). There were then 12 days of mixing followed by stable period of stratification
264 with onset the 14. June 2020 and a duration of 16 days until a mixing event around the 30. June 2020. The
265 following two weeks had cooler water and a mixed water column, hereafter a ca. 6 day period of
266 stratification from the 15. to 21. July 2020. A mixed phase of two weeks then followed until stratification
267 reestablished on 4. August 2020 and persisted until the end of August, partial mixing is indicated by the
268 buoy data from the 21. August 2020, but the weekly manual profile to deeper water indicate that full
269 mixing did not occur until after the 25. August 2020. The effects of the stratification and mixing events on
270 the high frequency DO data measured at -3.8 m are clear, with rapid deoxygenation occurring after the
271 onset of stratification and oxic bottom waters returning when the lake mixed (Fig, 2). The pattern in
272 chlorophyll-a also follow, to some degree, those of stratification, with the exception of early spring.
273 Chlorophyll-a values were extremely high in spring peaking at the start of June 2020 and falling gradually
274 (Fig. 2). ~~During the periods of stratification chlorophyll biomass was lower, likely limited by nitrogen~~
275 ~~(Søndergaard et al., 2023) and when a mixing even~~ During the periods of stratification chlorophyll
276 biomass was lower, and when a mixing event occurred the values increased, which is particularly evident
277 in the July mixing periods (Fig. 2).

278

279 **3.2 Concentrations of dissolved gases and fluxes from the surface waters.**

280 The concentrations of the dissolved gases showed great variation from near or below atmospheric
281 concentrations in some cases and up to an extremely high concentration (over 5 mg CH₄ C l⁻¹) in the
282 bottom waters on the 30. June 2020. There was some spatial heterogeneity in the surface waters, with the
283 more littoral locations showing the greatest variation and the highest values (Figs. 3,4,5). In particular the
284 most littoral zone, where the water was shallower around 1 m in depth, showed the highest values just
285 prior to, or ~~coincident~~ coincident with, the stratification turnover. Table 2 shows the mean diffusive flux of
286 each gas over the sampling period along with the mean flux in mixed and stratified phases. For CO₂ there
287 was a lot of temporal variation in flux dynamics, though not a large difference between mixed and

288 stratified phases in terms of mean values (Table 2). There were some periods of CO₂ influx in spring and
289 later summer and these tended to coincide with the end of a mixed phase and the start of the stratification
290 phase. Nitrous oxide concentrations were generally low (Figs 4 & 5) with the lake being a source of N₂O
291 in the spring period and a sink or a very small source thereafter. The CH₄ concentration in the surface
292 waters (Fig. 3) and the calculated diffusive emissions are relatively low, but did increase in the
293 stratification periods with higher average values (Table 2 & Fig. 6). There was also some spatial variation
294 with higher CO₂ and CH₄ diffusive emissions in the shallower sampling locations, both in stratified and
295 mixed conditions (Fig. 6).

296
297 The most marked patterns in GHG concentration were evident in the bottom waters sampled at -4.5 m,
298 which accumulated to very large concentrations of CO₂ but particularly CH₄ in the periods of
299 stratification (Fig. 3 & 4). The ratio of CO₂ to CH₄ is illustrative in highlighting how stratification has
300 altered the biogeochemical processes in the hypolimnion with CH₄ production becoming more prevalent. .
301 For example on 30. June 2020 after 16 days of stratification the the ratio CO₂:CH₄ in the bottom waters
302 was 0.8, whereas 7 days later after the mixing event it was 187 at the same depth.

303

304 **3.3 Ebullitive fluxes**

305 The CH₄ bubble flux ~~is~~, presented here as mean values for each of the 4 transects, ranged from 0.303 to
306 81.1 mg CH₄ C m² d⁻¹ for the individual transect over the growing season measurement. There is a very
307 clear, statistically significant impact of stratification on the ebullitive efflux of CH₄ with stratified periods
308 showing significantly markedly higher levels of emission (Fig. 7 and Table 2). In addition, there was a
309 difference in average emissions among the different transects, with those with lower average water depth
310 (T2 & T4) having lower emission than the transects with chambers over deeper water (T1 & T3) (Fig. 7).
311 The samples collected from the chambers reflect two weeks of bubble and diffusion collection and the
312 quantification of the flux is therefore an average of the period of chamber deployment, which was two

313 weeks, or in one case a single week (Fig. 7). This two week period on occasion covered both stratified
314 and mixed phases and on these occasions efflux was intermediate between purely mixed and stratified
315 periods (Table 2 and Fig. 7).

316

317 **3.4 Total lake fluxes**

318 Scaling up the results to total flux of gases from the whole lake over the period of study and including the
319 estimated emissions from two turnover events show a very different effect of stratification on the balance
320 of types of emissions for the three gases. The majority of CH₄ emission (56%) result from the two short-
321 lived turnover events (Fig. 8), whereas their contribution to CO₂ and N₂O emission was 5% and 1%
322 respectively.

323

324 Fluxes of CO₂ and N₂O were mostly diffusive, which represented 95% of emissions of both gases.
325 Methane diffusive flux was 14% of total emission, whereas CH₄ ebullition was more than twice as much
326 representing 29% of total CH₄ emission. In terms of global warming potential CO₂ and CH₄ emission
327 were comparable, but the contribution of the turnover efflux was the dominant factor for CH₄ emissions.

328

329 **4. Discussion**

330 The emission of the three GHGs showed great different degrees of variation between the mixed and
331 stratified phases. The largest and most significant variation was in CH₄ ebullition (Table 2), whilst the
332 difference in diffusive fluxes, though marked for CH₄ was not significant. The mean of the total emissions
333 from Ormstrup in the stratified phase (59.9 mg CH₄-C m⁻² day⁻¹) corresponds relatively closely to the
334 mean of the total emissions (ebullition plus diffusion) reported for lakes in this size range (47 mg CH₄-C
335 m⁻² day⁻¹) from a paper synthesising multiple studies (Rosentreter et al., 2021). The mean emissions for
336 the whole period (26.6 CH₄ -C m⁻² day⁻¹) were lower than Rosentreter et al. (2021) but similar to other
337 studies with mean emissions of 30.9, 20.7 and 22.7 CH₄ -C m⁻² day⁻¹ and were reported by Peacock et al.

338 (2021), Sørensen et al. (2023) and Peacock et al. (2019) respectively. Whereas the average CO₂ (504 mg CO₂-C
339 m⁻² day⁻¹) at Ormstrup was lower than 993.5 mg CO₂-C m⁻² day⁻¹ measured by Peacock et al. (2021) but
340 higher than the 264.6 and 205.1 mg CO₂-C m⁻² day⁻¹ measured by Sørensen et al. (2023) and Peacock et al.
341 (2019) respectively. The different temporal resolution and duration of these studies, eleven single day
342 sampling from April to December (Peacock et al., 2021), five days continuous sampling on one occasion
343 in late September (Sørensen et al., 2023) and a single early summer snapshot (Peacock et al., 2019) make direct
344 comparison difficult. The data here do, however, provide a clear answer to the question of how thermal
345 stratification affects GHG dynamics in shallow eutrophic lakes with an increase in total emissions
346 (diffusion, ebullition and turnover) during the stratified period (Table 2, Fig 9). Previous work, combining
347 observations and modelling suggested the opposite patterns (Bartosiewicz et al., 2019) as the shielding
348 effect of the stratification results in cooler bottom waters which reduces CH₄ production due to the
349 process being temperature dependent (Bartosiewicz et al., 2016). This strong shielding effect may apply
350 in deeper lakes experiencing more stable stratification, or less eutrophic lakes. The result here from a
351 relatively shallow eutrophic lake, indicate that temporary stratification causes increases in GHG
352 emissions.

353
354 Diffusive emissions did not, on average, show a strong stratification effect (Table 2). In particular
355 variation in N₂O emissions did not match patterns of stratification, with emissions more directly related to
356 nitrate concentrations (Audet et al., 2020), as reflected by the fact the lake is a sink of N₂O in late summer
357 when nitrate was below detection limits for several weeks. There were peaks in emission of CH₄ and CO₂
358 at the end of stratification periods, particularly in the shallower water sampling points (Fig. 6). There
359 were periods of influx of CO₂, which coincided somewhat with periods of stratification, but the pattern
360 was not consistent as other factors, for example, chlorophyll-a concentration also play a role.

361
362 Littoral zones can have markedly different GHG dynamics to deeper zones due to shallower water having
363 lower pressure (Wik et al., 2013), less time for CH₄ oxidation (Bastviken et al., 2008) or abundant plants

364 which influence a range of biogeochemical processes (Davidson et al., 2018; Esposito et al., 2023). It is
365 therefore possible that littoral zone dynamics could cause these differences. However, the increase
366 occurred at all three sampling points at the end of June 2020, which indicates a ~~more~~-lake-wide driver and
367 the peak may represent the start of mixing after stratification. Strong winds were measured on the 29th and
368 30th June 2020 (Søndergaard et al., 2023) coincident with these increased littoral emissions. These winds
369 would have caused lateral movement of the surface water causing an upwelling of bottom water, rich in
370 CH₄ and CO₂, in the littoral margins at the opposite end of the lake. Thus, whilst we do not have direct
371 evidence it seems more likely that these increased emissions in the littoral zone were ~~not~~-driven, at least
372 in part, by the partial mixing upwelling of the-GHG rich bottom waters.

373
374 In contrast to the diffusive flux, the ebullitive emission of CH₄ shows a very clear response to
375 stratification with an order of magnitude difference in emissions between periods where the sampling
376 reflected purely mixed or stratified periods (Table 2 & Fig. 7). The two-week resolution of the sampling
377 meant that some samples covered both stratified and mixed phases and these samples had intermediate
378 fluxes, as they cover both low (mixed) and high emission (stratified) periods. The spatial variation in
379 ebullition is also illustrative of the impacts of stratification and the role of anoxia in shaping CH₄ fluxes.
380 The two transects with the largest mean and maximum depths (T1 and T3) had the largest emissions, with
381 the deeper of the two (T1) having the highest emissions and they saw the greatest relative increase during
382 the stratification phases. This pattern is ~~the obverse of different to~~ that found in other studies where bubble
383 emissions were larger in shallower water ~~as higher pressure, although later in deeper location means~~
384 ~~production rates of CH₄ need to be higher for bubbles to form~~ the summer there was an increase in bubble
385 flux (Wik et al., 2013). ~~Deeper~~ The deeper water at Ormstrup ~~experiences~~ experienced anoxia earlier and
386 this appears to cause locations with deeper water to have higher ebullition rates than shallower areas. This
387 is at odds with ideas stemming from the metabolic theory of ecology stating that temperature (Yvon-
388 Durocher et al., 2014) in particular at the sediment surface (Bartosiewicz et al., 2019) can be used to
389 predict CH₄ efflux. Whilst it is a fact that CH₄ production is temperature dependent at the cellular level,

390 CH₄ emissions were rather independent of the sediment temperature, for example in the first two weeks of
391 July 2020 emissions were low and the sediment surface temperature was relatively high. Thus,
392 temperature alone is a poor predictor of ecosystem scale CH₄ emissions.

393
394 It should be noted that the methods used to estimate bubble flux here, where floating chambers are
395 sampled every two weeks is a “less than perfect method”, which in ~~most~~nearly all cases will
396 underestimate ebullitive flux. Logistical and financial constraints make continual sampling difficult and
397 here we balanced these constrains against the greater time required to apply more accurate methods, such
398 as bubble traps (Wik et al., 2013) ~~or~~, automatic flushing chambers (Bastviken et al., 2015). ~~Such is the~~
399 ~~variability of bubble flux in space and time that sampling campaigns covering days or weeks would~~
400 ~~potentially give an even more inaccurate picture of emissions than the method used here.~~ Such is the
401 variability of bubble flux in space and time that sampling campaigns covering days or weeks would
402 potentially give an even more inaccurate picture of emissions than the method used here (see
403 supplementary methods and supplementary materials). Though eddy covariance approaches offer a means
404 of continuous measurement capable of capturing short term changes and covering a large area (Erkkilä et
405 al., 2018). Thus, the continuous monitoring of ebullition using chambers with known biases was deemed
406 the least worst method available, but we acknowledge the caveat that ebullitive emissions may be
407 underestimated.

408
409 In addition to the diffusive and ebullitive emissions, the turnover flux, which consists of the gases
410 accumulated in the hypolimnion being released on turnover, was also estimated, with a correction of CH₄
411 oxidation applied. There were two major turnover events at the end of June and in late in August 2020,
412 which were preceded by 16 and 22 days of stratification, respectively. It was not possible to directly
413 measure turnover flux, as they are relatively discrete events where the efflux likely occurs over the course
414 of ~~just a few hours. Evidence of this is that the complete oxygenation of the water column during the~~
415 ~~mixing event at the start of July 2020 took just a few hours~~ (Søndergaard et al., 2023). ~~Thus, the efflux is~~

416 ~~estimated from the bottom concentration with the assumption that all the CO₂ and CH₄ in the bottom~~
417 ~~water was released at turnover, which is potentially an over estimate. Notwithstanding this uncertainty a~~
418 ~~few hours, or a few days. Thus, the efflux estimation is based on a series of assumptions and thus must be~~
419 ~~treated with caution. Notwithstanding this uncertainty,~~ we can be confident the turnover flux represents a
420 very large proportion of the total emission of CH₄ emissions from Ormstrup Lake over the growing
421 season. We estimate it contributed more than 50 % of growing season CH₄ emissions and 5 % of CO₂
422 emissions. This highlights a very significant, and ~~generally unmeasured~~ difficult to measure, contribution
423 to GHG emissions from lakes undergoing temporary stratification, which are among the most common
424 lake type in Denmark (Søndergaard, 2023 #8812).

425
426 The results here suggest that GHG dynamics were driven both directly and indirectly by the stratification
427 patterns and the anoxia it induced in the bottom waters. At Ormstrup Lake the thermal stratification of the
428 water column quickly led to anoxia, with only a matter of hours to days for the oxygen to be consumed
429 once the bottom waters were isolated (Fig. 2). The ratios of CO₂:CH₄ evidence how this promotes CH₄
430 over CO₂ production in the stratification phase (see Fig 9). In addition to promoting CH₄ production such
431 conditions would preclude, or severely limit, oxic CH₄ oxidation, which has the potential to consume a
432 large proportion of CH₄ produced in the anoxic sediments (Bastviken et al., 2008), though anoxic CH₄
433 can still occur (Blees et al., 2014). The raw emission data do not provide any direct information on the
434 balance of production versus oxidation, but the CO₂:CH₄ suggest there was marked shift to conditions
435 where methanogenesis was the dominant process and there was reduced CO₂ production. Studies have
436 shown that CH₄ oxidation can consume large proportions of the CH₄ produced under hypoxia (Saarela et
437 al., 2019) and it is possible that there is intense CH₄ oxidation occurring at the thermocline during the
438 periods of stratification at Ormstrup lake, but this was not directly measured at the lake. In addition to the
439 more direct effects of anoxia there may be some indirect effects of the patterns of stratification and
440 mixing that promote greater GHG emissions. Søndergaard et al. (2023) recently reported how nutrient
441 dynamics at Ormstrup Lake were altered by the lake stratification and full details can be found there, of

442 relevance here is the impact on chlorophyll-a which saw a large spring peak after which the abundance
443 tracked the stratification and mixing regime, with a lag time. There was a general reduction, or at least no
444 increase as the stratification period progressed, perhaps due to nutrient limitation in the epilimnion. Upon
445 mixing there was generally an increase in chlorophyll-a, though the weekly sampling resolution makes
446 this difficult to assess. Chlorophyll-a and the labile dissolved organic carbon (DOC) that result from
447 abundant chlorophyll-a have been shown to be associated with higher diffusive and ebullitive CH₄
448 emissions (Davidson et al., 2015; Beaulieu et al., 2019; West et al., 2012; Zhou et al., 2019). It is not
449 possible to say here whether a stable summer long stratification would have led to decreased chlorophyll-
450 a as nutrients became limiting due to their isolation in the bottom waters and reliable high frequency
451 chlorophyll-a data are required to convincingly demonstrate this phenomenon. Notwithstanding these
452 uncertainties it may be the case that the temporary stratification, interspersed with mixing events,
453 observed here represents a ‘sweet spot’ providing both the resources, i.e. chlorophyll-a and the labile
454 DOC it produces, and optimal conditions (anoxia) for CH₄ production.

455

456 Predicting climate change effects on GHG emissions in a future -warmer world is not straightforward, as
457 there are multiple interacting drivers which combine to shape the GHG emissions of lakes. However, this
458 study suggests that temporary stratification, which is increasingly recognised as prevalent in ponds and
459 shallow lakes (Holgerson et al., 2022) and is likely to become more common with continued climate
460 change impacts (Woolway and Merchant, 2019) is likely to increase GHG emissions. This will be
461 particularly the case in more eutrophic systems where abundance algal derived dissolved organic matter
462 can fuel CH₄ production (Zhou et al., 2019).

463

464 The combination of high frequency data on water temperature and dissolved oxygen combined with
465 weekly measurements of GHGs increase the reliability of the findings presented here. Up until relatively
466 recently it has been assumed that for shallow lakes, such as Ormstrup lake, stratification is not an
467 important feature. Sampling has therefore focused on the surface layers of water bodiess, using dissolved

468 concentrations of gases or floating chambers to characterise flux, e.g. (Davidson et al., 2015; Audet et al.,
469 2020; Peacock et al., 2021). Thus, most studies have overlooked bottom waters and do not have the
470 temporal resolution required to capture turnover flux emissions from surface measurements. Furthermore,
471 whilst many studies now include estimates of bubble emissions of CH₄ e.g. (Bergen et al., 2019), the
472 necessary temporal resolution to accurately characterise ebullitive emission is not well established. The
473 finding here indicated that in such dynamic systems near continuous measurement is desirable and that
474 short term collection over one or two days could provide massive, over or under estimate of CH₄
475 ebullition.

476
477 Our results show very large temporal variation in emissions of all three gases, but in particular CO₂ and
478 CH₄, and this highlights the need for high frequency measurements to accurately characterize emissions
479 from lakes. Even the weekly frequency of the sampling in this study was not sufficient to directly measure
480 all the emission pathways and turnover flux had to be inferred from bottom water calculations. These data
481 show that to capture the extent of GHG emissions from lakes it is vital we include all forms of flux,
482 including ebullition and turnover flux. Recent work has highlighted the fact that most emissions of CH₄
483 (over 50%) from fresh waters come from highly variable systems (Rosentreter et al., 2021), with the mean
484 and median emission rates of CH₄ differing greatly, indicating a few large emitters are responsible for a
485 large proportion of emissions. The sampling frequency applied here is rare, if a more standard resolution
486 of monthly measurements was applied the emissions estimate of all the gases, but in particular CH₄,
487 would be highly dependent on what phase of the stratification was captured. As an example, a monthly
488 sampling frequency could potentially miss all the stratification peaks - consequently massively
489 underestimating emissions, whereas a different sampling frequency could catch a number of peaks and
490 givinggive a much higher estimate. Thus, the same sampling frequency on the same lake, but timed
491 differently could lead to conclusions of highly variable emissions. ThusConsequently, it seems in these
492 highly dynamic systems that if temporarily where temporary stratification may occur in summer, high
493 frequency measurements are required to accurately estimate emissions. This is logistically challenging but

494 the current advances in the use of automatic flushing chambers (Bastviken et al., 2020) may provide the
495 potential for affordable high spatial and temporal resolution measurement of GHG dynamics. This is a
496 requisite for understanding the drivers of GHG dynamic, which is required for being able to predict how
497 they will respond in a range of scenarios related to land use, climate change and management
498 interventions.

499

500 **Code/data availability**

501 The datasets generated during and/or analysed during the current study are not publicly available as they
502 form part of ongoing research projects but are available from the corresponding author on reasonable
503 request and will be made publicly available later in the research project.

504

505 **Author contributions**

506 MS secured the funding for the wider lake restoration research project supplying the data. TAD, MS and
507 JA conceptualized the gas study. TAD and AN established the buoy and sensor system. EL, CE, TAD,
508 TB and JA collected and analysed the data. TAD wrote the paper and all authors commented on earlier
509 versions and read and approved the final draft.

510 **Competing interests**

511 The authors declare that they have no conflicts of interest.

512

513 **Acknowledgement**

514 We thanks our ~~er~~acksplendid technician team of Lene Vigh, Malene Kragh, Dorte Nedergaard and Dennis
515 Hansen for their extreme competence on the lab and the field. We acknowledge Theis Kragh for the depth
516 map of the lake already published in Søndergaard et al. 2023. We are very grateful to the Poul Due Jensen
517 Foundation for providing great support for this work and the Ormstrup project generally. TAD and CE
518 were also supported by GREENLAKES (No. 9040-00195B) and The European Union’s Horizon 2020
519 research and innovation programmes under grant agreement No 869296—The PONDERFUL Project.

520

521

522

523

524

525 Table 1. Summary lake information, summer mean values and (standard deviation) of a range of
 526 variables

Variable	n	Year
		2020
Secchi depth (m)	22	0.86 (0.28)
Chlorophyll a (µg/l)	<u>20</u>	53.4 (28.9)
pH	<u>22</u>	8.04 (0.77)
Total phosphorus (mg/l)	22	0.58 <u>(0.11)</u>
Total nitrogen (mg/l)	22	1.50 <u>(0.41)</u>

527

528 Table 2. Mean greenhouse gas flux (units CO₂: mg CO₂-C m⁻² day⁻¹, N₂O: mg N₂O -N m⁻² day⁻¹, CH₄ both
 529 diffusive and ebullitive in mg CH₄-C m⁻² day⁻¹) from the lake from spring to Autumn 2020. The emissions
 530 are divided in diffusive, ebullitive emissions. The mean values for all the surface water stations and all
 531 four transects of chambers are given. Emissions area separated into mixed versus stratified versus
 532 phases and there SD are also given. Ebullition iswas collected for a period covering two weeks so on a
 533 number of occasion covered both mixed and stratified periods and so forthus ebullition has a third
 534 category where both mixed and stratified conditions occurred is given. Ebullition was significantly
 535 different across the three phases, diffusive fluxes were not significantly different for p values of 0.05.

536

537

538

Emission type	gas	mean	mixed	Stratified	Strat and mixed
Diffusive	CO ₂	493.7 <i>(529.6)</i>	559.6 <i>(433.1)</i>	449.8 <i>(587.6)</i>	
	CH ₄	9.47 <i>(16.0)</i>	5.9 <i>(4.1)</i>	12.7 <i>(20.2)</i>	
	N ₂ O	0.11 <i>(0.09)</i>	0.09 <i>(0.08)</i>	0.12 <i>(0.11)</i>	
Ebullition	CH ₄	17.28 <i>(19.62)</i>	4.84 <i>(3.44)</i>	47.29 <i>(21.95)</i>	12.74 <i>(10.34)</i>

539

540

541 Figure legends

542 Figure 1. Ormstrup lake bathymetry and sampling stations for surface water greenhouse gas sampling
543 (St1, St2, St3) bottom waters were sampled at S3. Transects of 10 bubble traps were placed on T1- T4.
544 Adapted from the Søndergaard et al. 2023.

545 Figure 2 Temperature profile from June 2020 when the buoy was deployed and surface and bottom water
546 oxygen from June to the end of September 2020. Manual chlorophyll-a ($\mu\text{g L}^{-1}$) values are also given in
547 the top panel.

548 Figure 3. Dissolved CH_4 concentrations from surface and bottom waters – thermal stratification periods
549 highlighted in grey and the white background indicate mixed waters

550 Figure 4 . Dissolved CO_2 concentrations from surface and bottom waters–thermal stratification periods
551 highlighted in grey and the white background indicate mixed waters

552 Figure 5 Dissolved N_2O gas concentrations surface and bottom thermal stratification periods highlighted
553 in grey and the white background indicate mixed waters

554 Figure 6. Ormstrup ~~lakesurface~~lake surface fluxes of the CH_4 , CO_2 and N_2O gases based on dissolved
555 concentration , thermal stratification periods highlighted in grey and the white background indicate mixed
556 waters

557 Figure 7. Plot of CH_4 ebullition averaged for each transect (10 chambers per transect), data collected from
558 40 traps every two weeks. ~~thermal~~Thermal stratification periods highlighted in grey and the white
559 background indicate mixed waters.

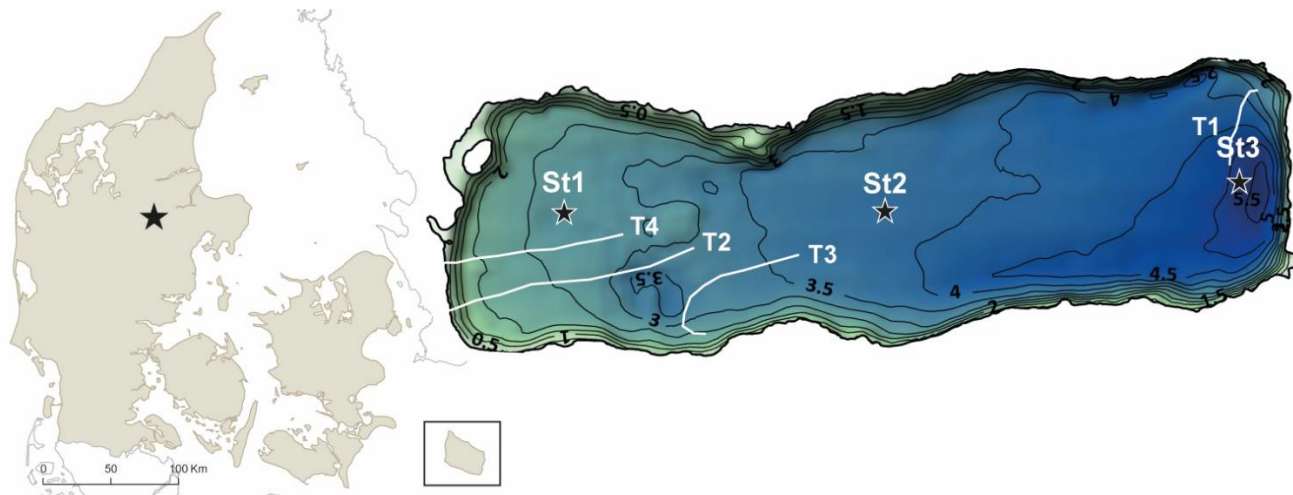
560 Figure 8 – Total lake emissions per gas over the growing ~~season~~season in CO_2 equivalents. The
561 emissions are divided different emission modes: Diffusive, ebullitive and turnover flux. All estimates
562 contain some uncertainty, in particular ebullitive flux is an underestimate and the turnover flux also
563 contains a gret deal of uncertainty.

564 Figure 9. Summary of the quantities of the gases present in the water and the ~~volumes emits~~volumes
565 emited from the different pathways. The size of the arrow is proportional to the emissions from each
566 pathway and with the stratified state on the left and the mixed state on the right, with the turnover flux in
567 the centre.

568

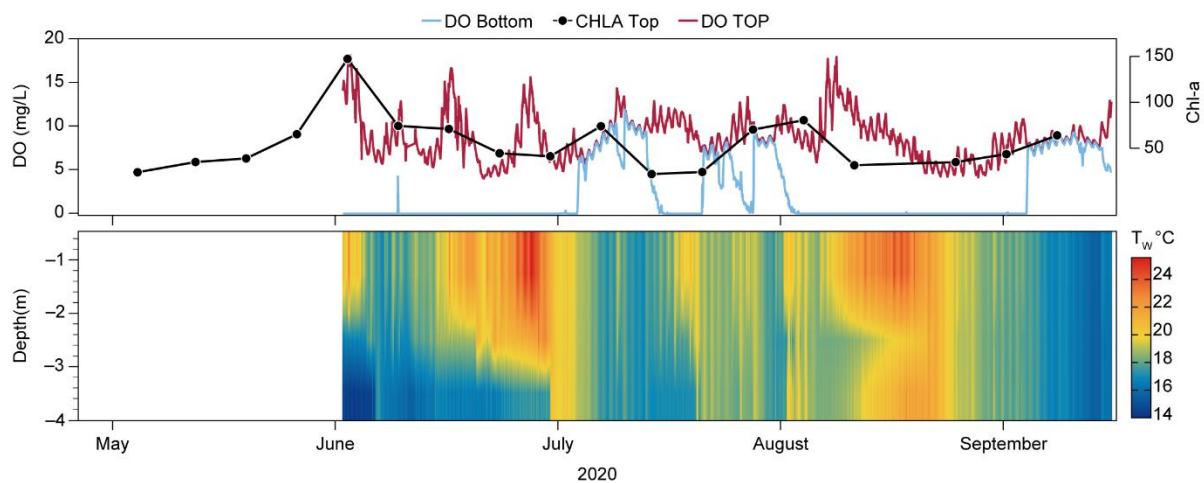
569 Figures and legends

570 Figure 1.



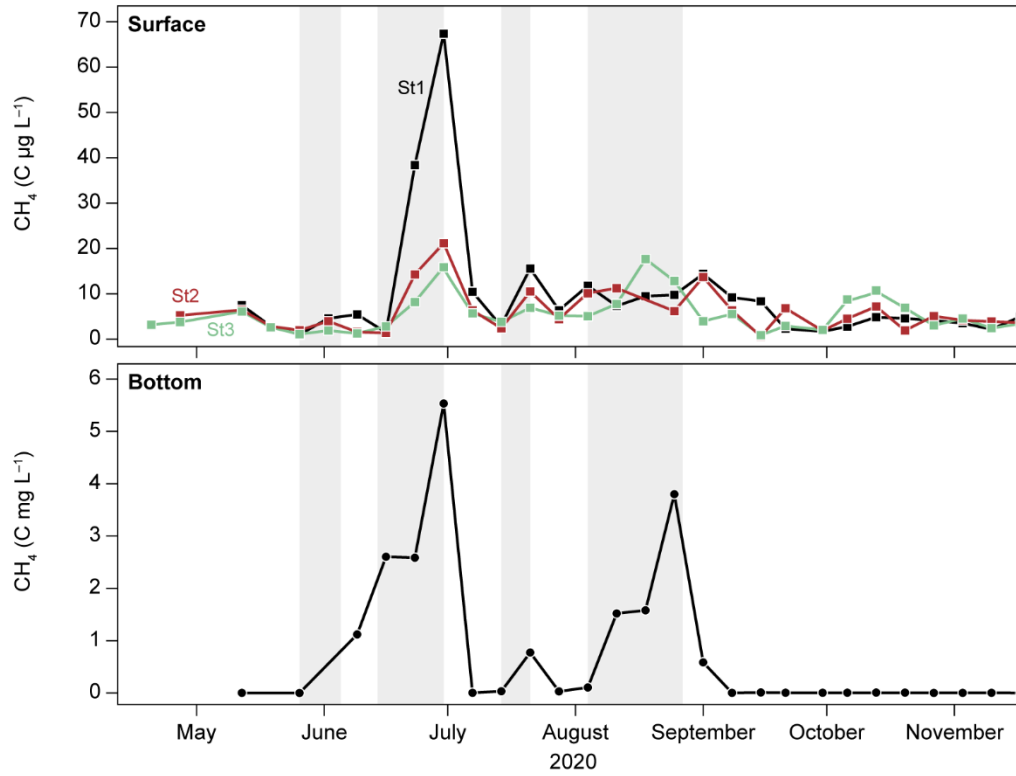
571
572 Figure 1. Ormstrup lake bathymetry and sampling stations for surface water greenhouse gas sampling (S1,
573 S2, S3) bottom waters were sampled at S3. Transects of 10 bubble traps were placed on T1- T4. Adapted
574 from the Søndergaard et al. 2023.

575



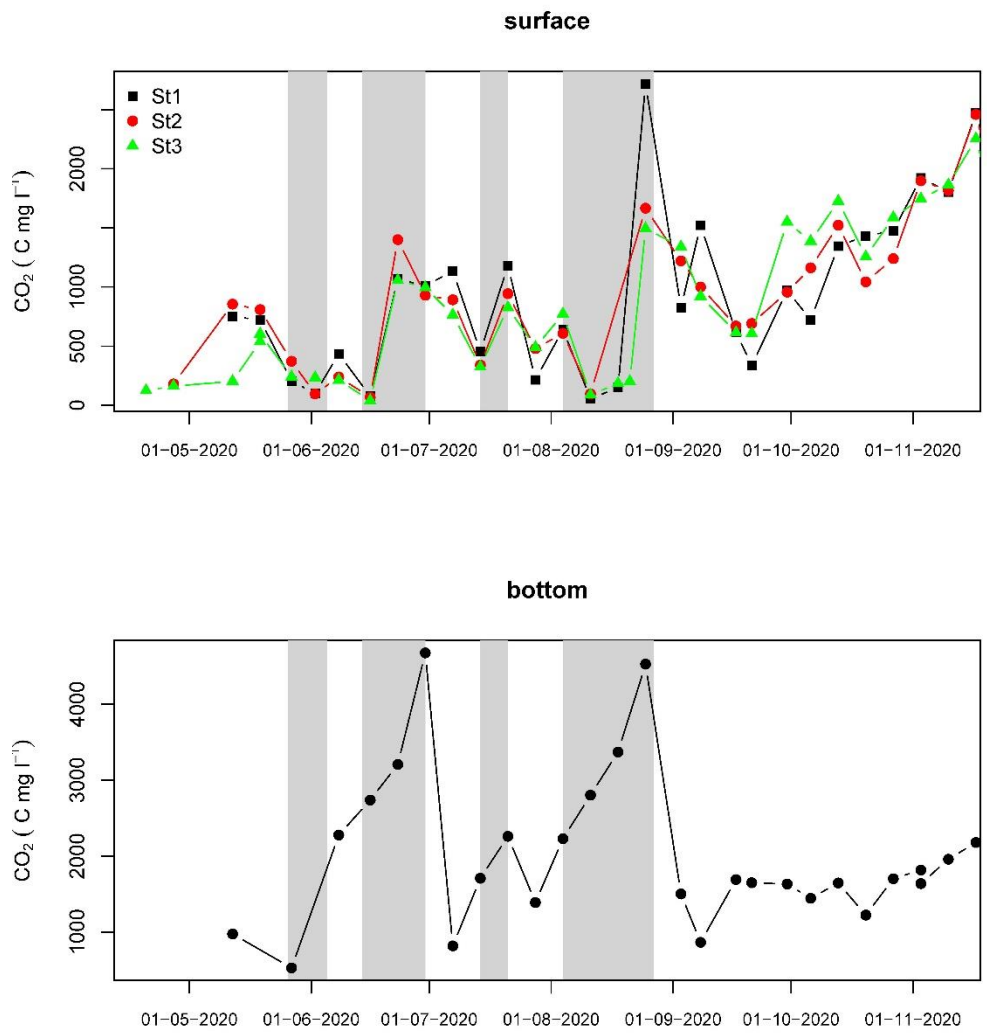
576
577 Figure 2 Temperature profile from June when the buoy was deployed and surface and bottom water
578 oxygen from June to the end of September. Chlorophyll-a ($\mu\text{g L}^{-1}$) values are also given in the top panel
579 and surface (DO TOP) and bottom (DO Bottom) dissolved oxygen (mg L^{-1}) are also given

580



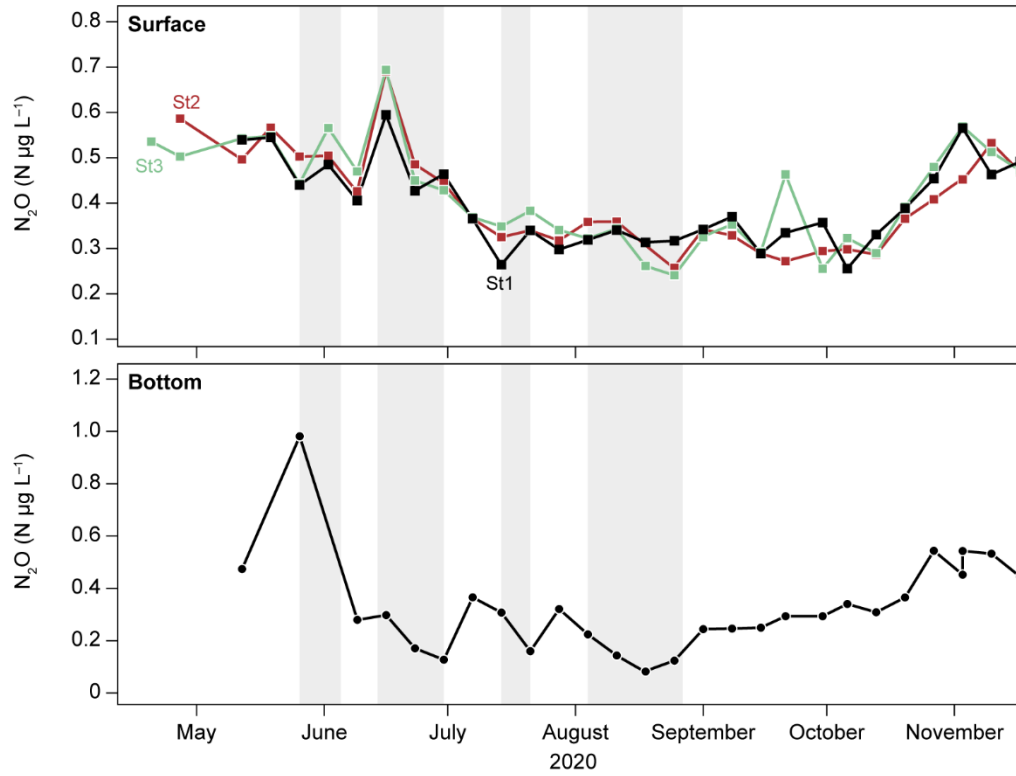
581

582 Figure 3. Dissolved CH₄ concentrations from surface and bottom waters – thermal stratification periods
 583 highlighted in grey; white background indicate mixed waters. Note different y axis scales



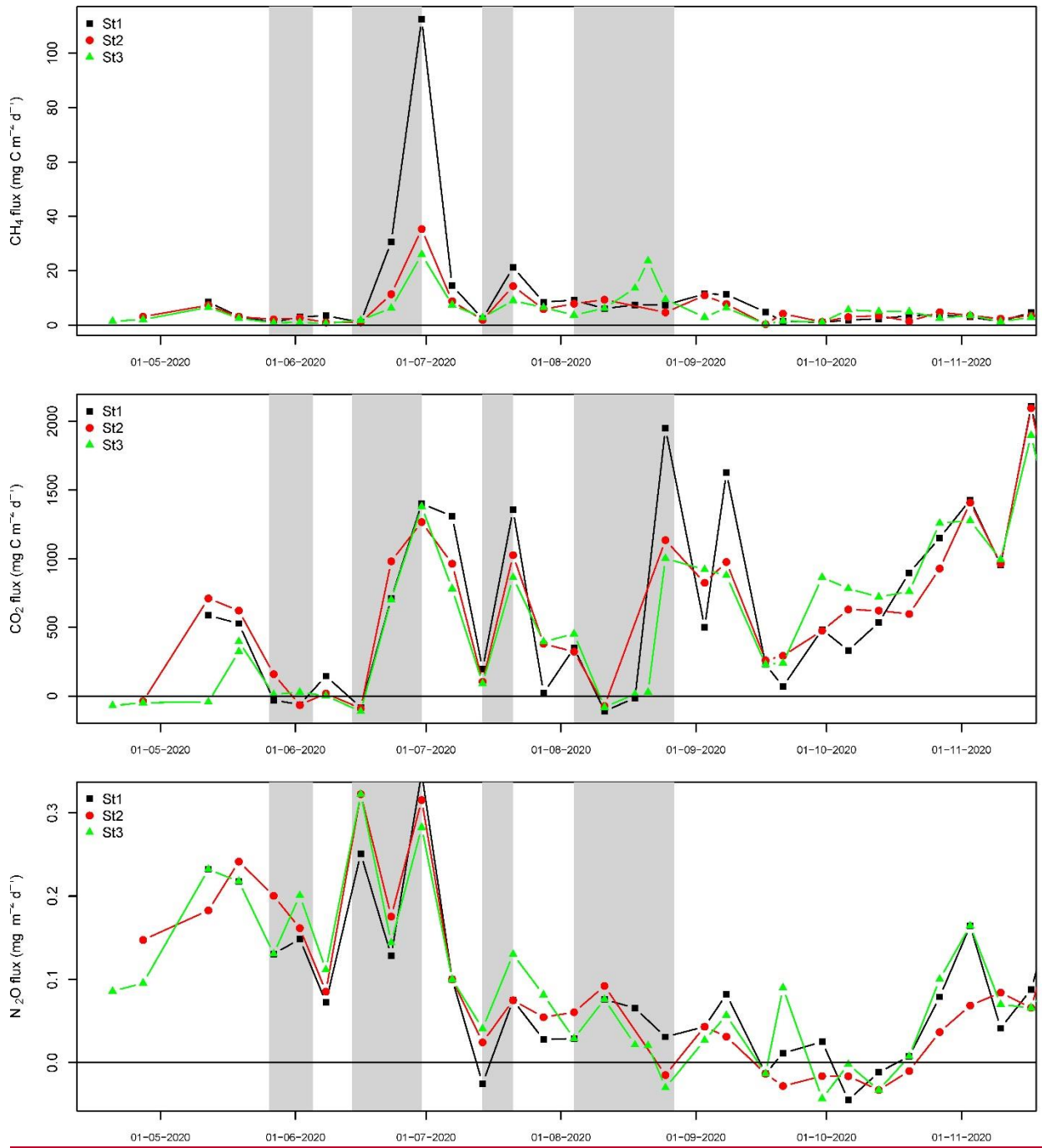
584

585 Figure 4 . Dissolved CO₂ concentrations from surface and bottom waters–
 586 thermal stratification periods highlighted in grey; white background indicate mixed waters



587

588 Figure 5 Dissolved N_2O gas concentrations surface and bottom thermal stratification periods highlighted
 589 in grey; white background indicate mixed waters

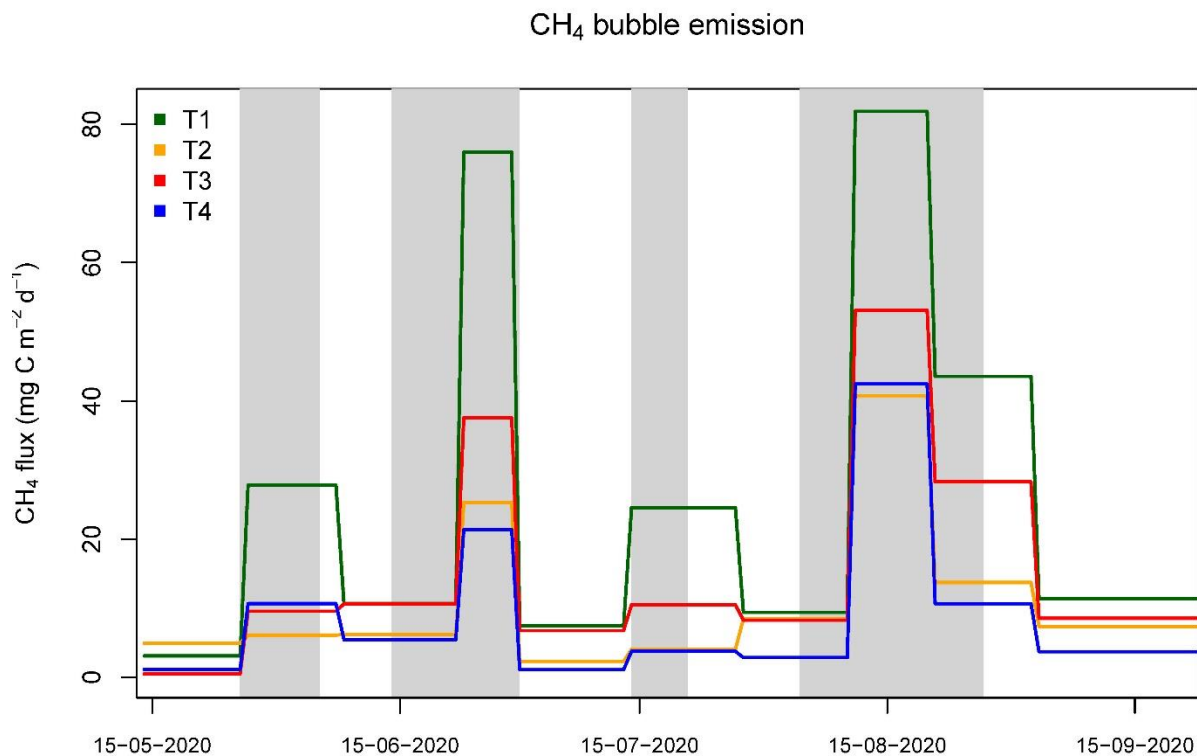


590

591 Figure 6. Omstrup lakesurface fluxes of the CH₄, CO₂ and N₂O gases based on dissolved concentration ,
 592 thermal stratification periods highlighted in grey; white background indicate mixed waters

593

594



595

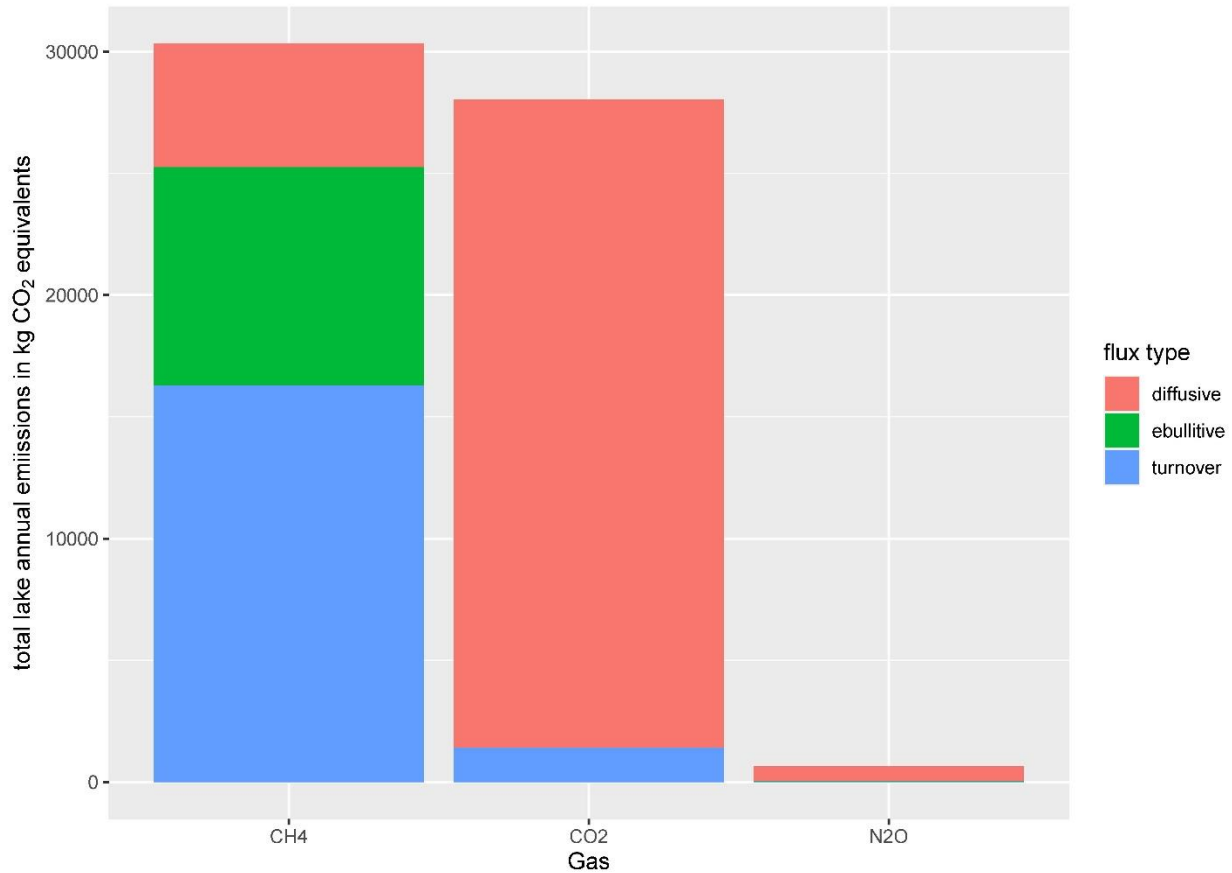
596 Figure 7. Plot of CH₄ ebullition averaged for each transect (10 chambers per transect), data collected from
597 40 traps every two weeks. thermal stratification periods highlighted in grey; white background indicate
598 mixed waters.

599

600

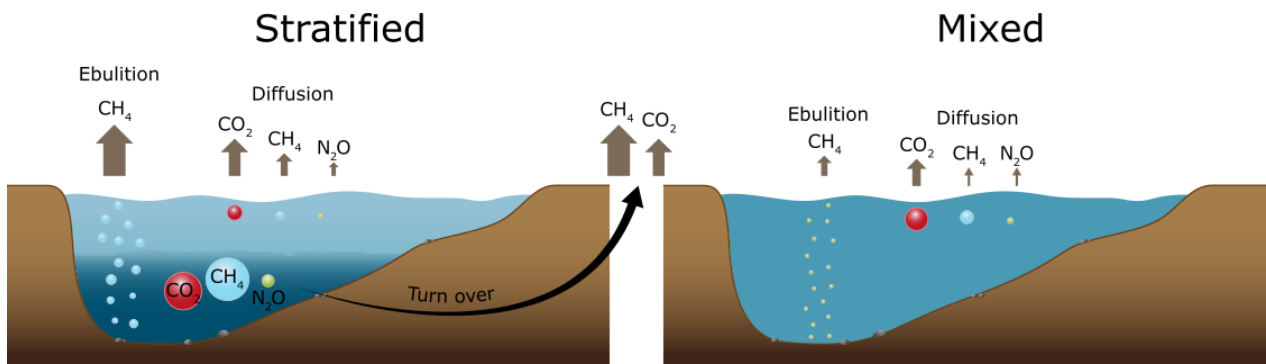
601

602



603
604
605
606
607

Figure 8 – Total lake emissions per gas over the growing season in CO₂ equivalents. The emissions are divided different emission pathways: Diffusive, ebullitive and turnover flux.



608
609
610
611

Figure 9 Summary of different flux types (bubble, diffusive and turnover) for the main greenhouse gases (CH₄ CO₂ and N₂O) observed between the stratified and mixed phases at Ormstrup lake patterns in the stratified and mixed phase. The turnover flux of CH₄ and CO₂ is also represented. The size of the arrow

612 represents the relative amount of emission and the size of the circle in the lake represents the
613 concentration of dissolved gases in stratified or mixed water column.

614

615

616 **References**

617 Aben, R. C. H., Barros, N., van Donk, E., Frenken, T., Hilt, S., Kazanjian, G., Lamers, L. P. M., Peeters, E. T.
618 H. M., Roelofs, J. G. M., de Senerpont Domis, L. N., Stephan, S., Velthuis, M., Van de Waal, D. B., Wik, M.,
619 Thornton, B. F., Wilkinson, J., DelSontro, T., and Kosten, S.: Cross continental increase in methane
620 ebullition under climate change, *Nat. Comms.*, 8, 1682, <https://doi.org/10.1038/s41467-017-01535-y>,
621 2017.

622 Audet, J., Carstensen, M. V., Hoffmann, C. C., Lavaux, L., Thiemer, K., and Davidson, T. A.: Greenhouse
623 gas emissions from urban ponds in Denmark, *Inland Waters*, 1-13,
624 <https://doi.org/10.1080/20442041.2020.1730680>, 2020.

625 Bartosiewicz, M., Laurion, I., and MacIntyre, S.: Greenhouse gas emission and storage in a small shallow
626 lake, *Hydrobiologia*, 757, 101-115, <https://doi.org/10.1007/s10750-015-2240-2>, 2015.

627 Bartosiewicz, M., Laurion, I., Clayer, F., and Maranger, R.: Heat-Wave Effects on Oxygen, Nutrients, and
628 Phytoplankton Can Alter Global Warming Potential of Gases Emitted from a Small Shallow Lake, *Environ.*
629 *Sci. Technol.*, 50, 6267-6275, <https://pubs.acs.org/doi/10.1021/acs.est.5b06312>, 2016.

630 Bartosiewicz, M., Przytulska, A., Lapierre, J.-F., Laurion, I., Lehmann, M. F., and Maranger, R.: Hot tops,
631 cold bottoms: Synergistic climate warming and shielding effects increase carbon burial in lakes, *Limnol.*
632 *Oceanogr. Lett.*, 4, 132-144, <https://doi.org/10.1002/lo.10117>, 2019.

633 Bastviken, D., Cole, J. J., Pace, M. L., and Van de Bogert, M. C.: Fates of methane from different lake
634 habitats: Connecting whole-lake budgets and CH₄ emissions, *J. Geophys. Res.*, 113, G02024,
635 <https://doi.org/10.1029/2007JG000608>, 2008.

636 Bastviken, D., Nygren, J., Schenk, J., Parellada Massana, R., and Duc, N. T.: Technical note: Facilitating the
637 use of low-cost methane (CH₄) sensors in flux chambers – calibration, data processing, and an open-
638 source make-it-yourself logger, *Biogeosciences*, 17, 3659-3667, [https://doi.org/10.5194/bg-17-3659-](https://doi.org/10.5194/bg-17-3659-2020)
639 [2020](https://doi.org/10.5194/bg-17-3659-2020), 2020.

640 Bastviken, D., Sundgren, I., Natchimuthu, S., Reyier, H., and Gålfalk, M.: Technical Note: Cost-efficient
641 approaches to measure carbon dioxide fluxes and concentrations in terrestrial and aquatic
642 environments using mini loggers, *Biogeosciences*, 12, 3849-3859, [https://doi.org/10.5194/bg-12-3849-](https://doi.org/10.5194/bg-12-3849-2015)
643 [2015](https://doi.org/10.5194/bg-12-3849-2015), 2015.

644 Bastviken, D., Treat, C. C., Pangala, S. R., Gauci, V., Enrich-Prast, A., Karlson, M., Gålfalk, M., Romano, M.
645 B., and Sawakuchi, H. O.: The importance of plants for methane emission at the ecosystem scale, *Aquat.*
646 *Bot.*, 184, 103596, <https://doi.org/10.1016/j.aquabot.2022.103596>, 2023.

647 Beaulieu, J. J., DelSontro, T., and Downing, J. A.: Eutrophication will increase methane emissions from
648 lakes and impoundments during the 21st century, *Nat. Comms.*, 10, 1-5,
649 <https://doi.org/10.1038/s41467-019-09100-5>, 2019.

650 Bergen, T. J. H. M., Barros, N., Mendonça, R., Aben, R. C. H., Althuisen, I. H. J., Huszar, V., Lamers, L. P.
651 M., Lürling, M., Roland, F., and Kosten, S.: Seasonal and diel variation in greenhouse gas emissions from
652 an urban pond and its major drivers, *Limnol. Oceanogr.*, 64, 2129-2139,
653 <https://doi.org/10.1002/lno.11173>, 2019.

654 Blees, J., Niemann, H., Wenk, C. B., Zopfi, J., Schubert, C. J., Kirf, M. K., Veronesi, M. L., Hitz, C., and
655 Lehmann, M. F.: Micro-aerobic bacterial methane oxidation in the chemocline and anoxic water column
656 of deep south-Alpine Lake Lugano (Switzerland), *Limnol. Oceanogr.*, 59, 311-324,
657 <https://doi.org/10.4319/lo.2014.59.2.0311>, 2014.

658 Cole, J.: Freshwater in flux, *Nat. Geosci.*, 6, 13-14, <https://doi.org/10.1038/ngeo1696>, 2013.

659 Cole, J. J. and Caraco, N. F.: Atmospheric exchange of carbon dioxide in a low-wind oligotrophic lake
660 measured by the addition of SF₆, *Limnol. Oceanogr.*, 43, 647-656,
661 <https://doi.org/10.4319/lo.1998.43.4.0647>, 1998.

662 Davidson, T. A., Audet, J., Jeppesen, E., Landkildehus, F., Lauridsen, T. L., Søndergaard, M., and
663 Syvaranta, J.: Synergy between nutrients and warming enhances methane ebullition from experimental
664 lakes, *Nat. Clim. Chang.*, 8, 156-160, <https://doi.org/10.1038/s41558-017-0063-z>, 2018.

665 Davidson, T. A., Audet, J., Svenning, J.-C. C., Lauridsen, T. L., Søndergaard, M., Landkildehus, F., Larsen, S.
666 E., and Jeppesen, E.: Eutrophication effects on greenhouse gas fluxes from shallow-lake mesocosms
667 override those of climate warming, *Glob. Chang. Biol.*, 21, 4449-4463,
668 <https://doi.org/10.1111/gcb.13062>, 2015.

669 Deacon, E. L.: Sea-air gas transfer: The wind speed dependence, *Bound.- Layer. Meteorol.*, 21, 31-37,
670 <https://doi.org/10.1007/bf00119365>, 1981.

671 Deemer, B. R. and Holgerson, M. A.: Drivers of Methane Flux Differ Between Lakes and Reservoirs,
672 Complicating Global Upscaling Efforts, *J. Geophys. Res. Biogeosci.* . 126, e2019JG005600,
673 <https://doi.org/10.1029/2019JG005600>, 2021.

674 DelSontro, T., Boutet, L., St-Pierre, A., del Giorgio, P. A., and Prairie, Y. T.: Methane ebullition and
675 diffusion from northern ponds and lakes regulated by the interaction between temperature and system
676 productivity, *Limnol. Oceanogr.*, 61, S62-S77, <http://doi.wiley.com/10.1002/lno.10335>, 2016.

677 Duc, N. T., Silverstein, S., Lundmark, L., Reyier, H., Crill, P., and Bastviken, D.: Automated flux chamber
678 for investigating gas flux at water–air interfaces, *Environ. Sci. Technol.*, 47, 968-975, 2013.

679 Erkkilä, K. M., Ojala, A., Bastviken, D., Biermann, T., Heiskanen, J. J., Lindroth, A., Peltola, O., Rantakari,
680 M., Vesala, T., and Mammarella, I.: Methane and carbon dioxide fluxes over a lake: comparison between
681 eddy covariance, floating chambers and boundary layer method, *Biogeosciences*, 15, 429-445,
682 10.5194/bg-15-429-2018, 2018.

683 Esposito, C., Nijman, T. P. A., Veraart, A. J., Audet, J., Levi, E. E., Lauridsen, T. L., and Davidson, T. A.:
684 Activity and abundance of methane-oxidizing bacteria on plants in experimental lakes subjected to
685 different nutrient and warming treatments, *Aquat. Bot.*, 185, 103610,
686 <https://doi.org/10.1016/j.aquabot.2022.103610>, 2023.

687 Holgerson, M. A., Richardson, D. C., Roith, J., Bortolotti, L. E., Finlay, K., Hornbach, D. J., Gurung, K., Ness,
688 A., Andersen, M. R., Bansal, S., Finlay, J. C., Cianci-Gaskill, J. A., Hahn, S., Janke, B. D., McDonald, C.,
689 Mesman, J. P., North, R. L., Roberts, C. O., Sweetman, J. N., and Webb, J. R.: Classifying Mixing Regimes
690 in Ponds and Shallow Lakes, *Water Resour. Res.*, 58, e2022WR032522,
691 <https://doi.org/10.1029/2022WR032522>, 2022.

692 Jespersen, A. and Christoffersen, K.: Measurements of Chlorophyll a from phytoplankton using ethanol
693 as extraction solvent., *Archiv für Hydrobiologie*, 109, 445-454, 1987.

694 Kirillin, G. and Shatwell, T.: Generalized scaling of seasonal thermal stratification in lakes, *Earth Sci. Rev.*,
695 161, 179-190, <https://doi.org/10.1016/j.earscirev.2016.08.008>, 2016.

696 Koschorreck, M., Prairie, Y. T., Kim, J., and Marcé, R.: Technical note: CO₂ is not like CH₄ – limits of and
697 corrections to the headspace method to analyse pCO₂ in fresh water, *Biogeosciences*, 18, 1619-1627,
698 10.5194/bg-18-1619-2021, 2021.

699 McAuliffe, C.: Gas chromatographic determination of solutes by multiple phase equilibrium, *Chem*
700 *Technol*, 1, 46-51, 1971.

701 Meerhoff, M., Audet, J., Davidson, T. A., De Meester, L., Hilt, S., Kosten, S., Liu, Z., Mazzeo, N., Paerl, H.,
702 Scheffer, M., and Jeppesen, E.: Feedbacks between climate change and eutrophication: revisiting the
703 allied attack concept and how to strike back, *Inland Waters*, 1-42,
704 <https://doi.org/10.1080/20442041.2022.2029317>, 2022.

705 Peacock, M., Audet, J., Jordan, S., Smeds, J., and Wallin, M. B.: Greenhouse gas emissions from urban
706 ponds are driven by nutrient status and hydrology, *Ecosphere*, 10, e02643,
707 <https://doi.org/10.1002/ecs2.2643>, 2019.

708 Peacock, M., Audet, J., Bastviken, D., Cook, S., Evans, C. D., Grinham, A., Holgerson, M. A., Högbom, L.,
709 Pickard, A. E., Zieliński, P., and Futter, M. N.: Small artificial waterbodies are widespread and persistent

710 emitters of methane and carbon dioxide, *Glob. Chang. Biol.*, 27, 5109-5123,
711 <https://doi.org/10.1111/gcb.15762>, 2021.

712 Petersen, S. O., Hoffmann, C. C., Schäfer, C. M., Blicher-Mathiesen, G., Elsgaard, L., Kristensen, K.,
713 Larsen, S. E., Torp, S. B., and Greve, M. H.: Annual emissions of CH₄ and N₂O, and ecosystem respiration,
714 from eight organic soils in Western Denmark managed by agriculture, *Biogeosciences*, 9, 403-422,
715 <https://doi.org/10.5194/bg-9-403-2012>, 2012.

716 Pinheiro, J., Bates, D., DebRoy, S., Sarkar, D., and R Core Team: *nlme: Linear and Nonlinear Mixed Effects*
717 *Models*, 2014.

718 R Development Core Team: *R: a language and environment for statistical computing*. R Foundation for
719 Statistical Computing (4.2.1) [code], 2022.

720 Rosentreter, J. A., Borges, A. V., Deemer, B. R., Holgerson, M. A., Liu, S., Song, C., Melack, J., Raymond, P.
721 A., Duarte, C. M., Allen, G. H., Olefeldt, D., Poulter, B., Battin, T. I., and Eyre, B. D.: Half of global methane
722 emissions come from highly variable aquatic ecosystem sources, *Nat. Geosci.*, 14, 225-230,
723 <https://doi.org/10.1038/s41561-021-00715-2>, 2021.

724 Saarela, T., Rissanen, A. J., Ojala, A., Pumpanen, J., Aalto, S. L., Tirola, M., Vesala, T., and Jäntti, H.: CH₄
725 oxidation in a boreal lake during the development of hypolimnetic hypoxia, *Aquat. Sci.*, 82, 19,
726 <https://doi.org/10.1007/s00027-019-0690-8>, 2019.

727 Schubert, C. J., Diem, T., and Eugster, W.: Methane Emissions from a Small Wind Shielded Lake
728 Determined by Eddy Covariance, Flux Chambers, Anchored Funnels, and Boundary Model Calculations: A
729 Comparison, *Environ. Sci. Technol.*, 46, 4515-4522, <https://doi.org/10.1021/es203465x>, 2012.

730 Sørensen, J. S., Sand-Jensen, K., Martinsen, K. T., Polauke, E., Kjær, J. E., Reitzel, K., and Kragh, T.: Methane and
731 carbon dioxide fluxes at high spatiotemporal resolution from a small temperate lake, *Sci. Total Environ.*,
732 878, 162895, <https://doi.org/10.1016/j.scitotenv.2023.162895>, 2023.

733 Søndergaard, M., Jeppesen, E., Peder Jensen, J., and Lildal Amsinck, S.: Water Framework Directive:
734 ecological classification of Danish lakes, *J. Appl. Ecol.*, 42, 616-629, <https://doi.org/10.1111/j.1365-2664.2005.01040.x>, 2005.

735 Søndergaard, M., Nielsen, A., Skov, C., Baktoft, H., Reitzel, K., Kragh, T., and Davidson, T. A.: Temporarily
736 and frequently occurring summer stratification and its effects on nutrient dynamics, greenhouse gas
737 emission and fish habitat use: case study from Lake Ormstrup (Denmark), *Hydrobiologia*, 850, 65-79,
738 <https://doi.org/10.1007/s10750-022-05039-9>, 2023.

740 Thottathil, S. D., Reis, P. C. J., and Prairie, Y. T.: Methane oxidation kinetics in northern freshwater lakes,
741 *Biogeochemistry*, 143, 105-116, [10.1007/s10533-019-00552-x](https://doi.org/10.1007/s10533-019-00552-x), 2019.

742 Wanninkhof, R.: Relationship between wind-speed and gas-exchange over the ocean, *J. Geophys. Res.*
743 *Oceans*, 97, 7373-7382, <https://doi.org/10.1029/92jc00188>, 1992.

744 Weiss, R. F.: Carbon dioxide in water and seawater: the solubility of a non-ideal gas, *Mar. Chem.*, 2, 203-
745 215, [https://doi.org/10.1016/0304-4203\(74\)90015-2](https://doi.org/10.1016/0304-4203(74)90015-2), 1974.

746 Weiss, R. F. and Price, B. A.: Nitrous oxide solubility in water and seawater, *Mar. Chem.*, 8, 347-359,
747 [https://doi.org/10.1016/0304-4203\(80\)90024-9](https://doi.org/10.1016/0304-4203(80)90024-9), 1980.

748 West, W. E., Coloso, J. J., and Jones, S. E.: Effects of algal and terrestrial carbon on methane production
749 rates and methanogen community structure in a temperate lake sediment, *Freshw. Biol.*, 57, 949-955,
750 <https://doi.org/10.1111/j.1365-2427.2012.02755.x>, 2012.

751 Wiesenburg, D. A. and Guinasso, N. L.: Equilibrium solubilities of methane, carbon monoxide, and
752 hydrogen in water and sea water, *J. Chem. Eng. Data* . 24, 356-360,
753 <https://doi.org/10.1021/je60083a006>, 1979.

754 Wik, M., Crill, P. M., Varner, R. K., and Bastviken, D.: Multiyear measurements of ebullitive methane flux
755 from three subarctic lakes, *J. Geophys. Res. Biogeosci.* . 118, 1307-1321,
756 <https://doi.org/10.1002/jgrg.20103>, 2013.

757 Woolway, R. I. and Merchant, C. J.: Worldwide alteration of lake mixing regimes in response to climate
758 change, *Nat. Geosci.*, 12, 271-276, <https://doi.org/10.1038/s41561-019-0322-x>, 2019.

759 Yvon-Durocher, G., Allen, A. P., Montoya, J. M., Trimmer, M., and Woodward, G.: The temperature
760 dependence of the carbon cycle in aquatic ecosystems, *Adv. Ecol. Res.*, 43, 267-313,
761 <https://doi.org/10.1016/B978-0-12-385005-8.00007-1>, 2010.

762 Yvon-Durocher, G., Allen, A. P., Bastviken, D., Conrad, R., Gudas, C., St-Pierre, A., Thanh-Duc, N., and del
763 Giorgio, P. A.: Methane fluxes show consistent temperature dependence across microbial to ecosystem
764 scales, *Nature*, 507, 488-491, <https://doi.org/10.1038/nature13164>, 2014.

765 Zhou, Y., Zhou, L., Zhang, Y., de Souza, J. G., Podgorski, D. C., Spencer, R. G. M., Jeppesen, E., and
766 Davidson, T. A.: Autochthonous dissolved organic matter potentially fuels methane ebullition from
767 experimental lakes, *Water Res.*, 166, 115048, <https://doi.org/10.1016/j.watres.2019.115048>, 2019.

768